

Original article

Marcus W. Ott, Christian Dietz, Simon Trosien*, Sabrina Mehlhase, Martin J. Bitsch, Maximilian Nau, Tobias Meckel, Andreas Geissler, Gregor Siegert, Jasmin Huong, Brigitte Hertel, Robert W. Stark and Markus Biesalski*

Co-curing of epoxy resins with aminated lignins: insights into the role of lignin homo crosslinking during lignin amination on the elastic properties

https://doi.org/10.1515/hf-2020-0060 Received March 5, 2020; accepted July 1, 2020; published online August 25, 2020

Abstract: To improve the reactivity of lignin for incorporation into high value polymers, the introduction of amines via Mannich reaction is a commonly used strategy. During this functionalization reaction, intra- as well as intermolecular lignin-lignin crosslinking occurs, which can vastly change the elastic properties of the lignin, and therefore, the properties of the resulting polymer. Therefore, the molecular structure of the amine that is used for such a lignin functionalization may be of great importance. However, the relationship between the molecular structure of the amine and the elastic properties of the lignin-based polymer that is generated thereof, has not been fully understood. Herein, this relationship was investigated in detail and it was observed that the molecular flexibility of the amines plays a predominant role: The use of more

Marcus W. Ott and Christian Dietz: These authors contributed equally as first authors.

*Corresponding authors: Markus Biesalski, Laboratory of Macromolecular Chemistry and Paper Chemistry, Technical University of Darmstadt, Alarich-Weiss-Str. 8, 64287 Darmstadt, Germany, E-mail: biesalski@tu-darmstadt.de; and Simon Trosien, Laboratory of Macromolecular Chemistry and Paper Chemistry, Technical University of Darmstadt, Alarich-Weiss-Str. 8, 64287 Darmstadt, Germany. https://orcid.org/0000-0001-6662-0673

Marcus W. Ott, Sabrina Mehlhase, Martin J. Bitsch, Maximilian Nau, Tobias Meckel, Andreas Geissler, Gregor Siegert and Jasmin Huong, Laboratory of Macromolecular Chemistry and Paper Chemistry, Technical University of Darmstadt, Alarich-Weiss-Str. 8, 64287 Darmstadt, Germany. https://orcid.org/0000-0003-0759-2072 (T. Meckel)

Christian Dietz and Robert W. Stark, Physics of Surfaces, Institute of Material Science, Technical University of Darmstadt, Alarich-Weiss-Str. 16, 64287 Darmstadt, Germany. https://orcid.org/0000-0002-4134-7516 (C. Dietz). https://orcid.org/0000-0001-8678-8449 (R.W. Stark)

Brigitte Hertel, Institute of Biology, Technical University of Darmstadt, Schnittspahnstraße. 4, 64287 Darmstadt, Germany

flexible amines results in an increase in elasticity and the use of less flexible amines yields more rigid resin material. In addition to the macroscopic 3-point bending flexural tests, the elastic modules of the resins were determined on the nanometer scale by using atomic force microscopy (AFM) in the PeakForce tapping modus. Thus, it could be demonstrated that the intrinsic elasticities of the lignin domains are the main reason for the observed tendency.

Keywords: ammoniated lignin; homo crosslinking; kraft lignin; lignin amination; mechanical properties; structure–property relationship.

1 Introduction

Lignin is one of the most abundant biopolymers on Earth. Annually, an estimated amount of 63 billion tons of lignin is newly formed in nature (Türk 2014). 50 million tons of lignin are generated as a by-product in the pulp and paper industry, mainly obtained through the so-called "kraft process", which makes it cost-effective and highly available (Türk 2014). However, at present the majority of this biomolecule is combusted for energy production although its unique chemical structure provides a great potential for many fields of application (Laurichesse and Avérous 2014). For example, lignin exhibits various reactive groups for chemical modification (e.g., different types of hydroxyl groups and arene moieties), (Crestini et al. 2017), which makes it valuable for the synthesis of polymeric materials (Laurichesse and Avérous 2014; Sun et al. 2018; Upton and Kasko 2016). Thereby, lignin can be used either as a filler which is bound electrostatically (as well as by hydrogen bonds) or it can be chemically incorporated via covalent bond formation, where lignin acts as a cross-linker to other components. The latter idea, i.e. utilizing lignin as a macromonomer for plastics, is more than 50 years old and a plethora of approaches to implement lignin into polymeric materials has been established (Hofmann and Glasser

2006; Newmann and Glasser 1985; Ragauskas et al. 2014). Examples range from bio-based polyesters (Guo et al. 1992; Guo and Gandini 1991), to polyurethanes (Moorer et al. 1970; Zieglowski et al. 2019), phenol formaldehyde resins (Danielson and Simonson 1998; Tejado et al. 2007) and epoxy resins (Auvergne et al. 2014; Ding and Matharu 2014), to name only the most prominent. For preparation of the latter class of polymeric materials, the lignin can either be equipped with oxirane moieties and used as epoxy compound (Gioia et al. 2018; Nieh and Glasser 1989; Zhao et al. 2018) or it can be used as nucleophilic curing agent. Although lignin intrinsically carries nucleophilic hydroxyl groups, which in principle could be suitable for curing of an epoxy-functional compound, there are only a few articles describing the use of unmodified lignin for this particular purpose. Up to now, only very specialized lignins (e.g. steam-exploded bamboo lignin) were used (Sasaki et al. 2013). The main reason attributes to the fact that hydroxyl groups are relatively weak nucleophiles. In order to transform lignin into a stronger nucleophile, prefunctionalization with reactive amines can be a useful strategy (Jiang et al. 2013; Pan et al. 2013; Sun et al. 2017). A convenient approach to accomplish this transformation is the treatment of the arene cores of lignin with diamines via Mannich reaction (Brezny et al. 1988). Thereby, mechanistically, an iminium ion (Mannich base) is generated as condensation product of an amine and formaldehyde, respectively. This imine is further capable to undergo an electrophilic reaction at the electron-rich guaiacyl and p-hydroxyphenyl moieties of lignin (Mikawa et al. 1956). Note, if the Mannich reaction takes place in ortho position of a hydroxyl group by using a primary amine and if furthermore an excess of formaldehyde is present, a cyclization reaction can occur, which leads to the formation of benzoxazine derivatives (Scheme 1) (Abarro et al. 2016; Burke 1949; Laobuthee et al. 2001; Phalak et al. 2017).

The functionalization of lignin via Mannich reaction was first described by Brežný in 1988, when studying the reaction

Scheme 1: Amination of lignin via Mannich reaction with excess of formaldehyde. Note that if the amine provides a NHR instead of a NH₂ group, no benzoxazine structure can be formed. For clarity, only the benzoxazine structures are shown.

of lignin with amino acids (Brezny et al. 1988). In the following, the modification method was extended to functionalize lignin with a variety of compounds (methyl and dimethylamine (Ge et al. 2015), DETA (diethylenetriamine) (Liu et al. 2013; Yue et al. 2011), TETA (triethylenetetramine) (Mendis et al. 2015), diethanolamine (Ding et al. 2014), urea (Zhang et al. 2012), etc.). However, during the amination reaction homo crosslinking can occur besides generating nucleophilic amino functionalities. Crosslinking can directly influence the flexibility of the lignin molecules, and thus, the elastic properties of any lignin-based polymer synthesized with such modified compounds. The crosslinking reaction is highly complex and depends on various parameters. Amongst others, of particular relevance are molecular effects, i.e. the reactivity of the amine, steric accessibility as well as molecular flexibility of the amine molecules themselves, which are bound to the lignin. However, the influence of the molecular structure of the lignin-bound amine on the mechanical properties of the polymeric material made thereof has not yet been investigated.

Herein, the influence of the molecular structure of the diamine that is used for lignin amination on the elastic properties of the resulting materials was investigated. To this end, different aminated lignin derivatives were synthesized, used for curing of a model epoxy resin formulation and analyzed with respect to the mechanical properties of the cured material.

2 Materials and methods

2.1 Chemicals

All chemicals and solvents were purchased from Fisher Scientific, Sigma-Aldrich and Alfa Aesar and used as received unless otherwise stated. For silicon molds, Elastosil M4645 A/B was used and supplied by Reiff GmbH. Epoxy resin matrix EPOSID 2031 (EEW = 180-190) and hardener EPODUR VP664 (AE = 58) (Duroplast Chemie, Germany) were used.

2.2 Lignin

Softwood kraft lignin commercially available BioPivaTM 100 from UPM Biochemicals was used for all experiments. Dry content: 99%; $Mn = 1946 \text{ g mol}^{-1}$; $Mw = 4593 \text{ g mol}^{-1}$.

2.3 Pretreatment of lignin for comparison of the analytical data

In order to better compare spectra of non-aminated lignin with spectra of aminated lignin, the crude lignin has been treated under the same conditions as are present during the amination (see general protocol of lignin amination). In this way, low and very high molecular weight

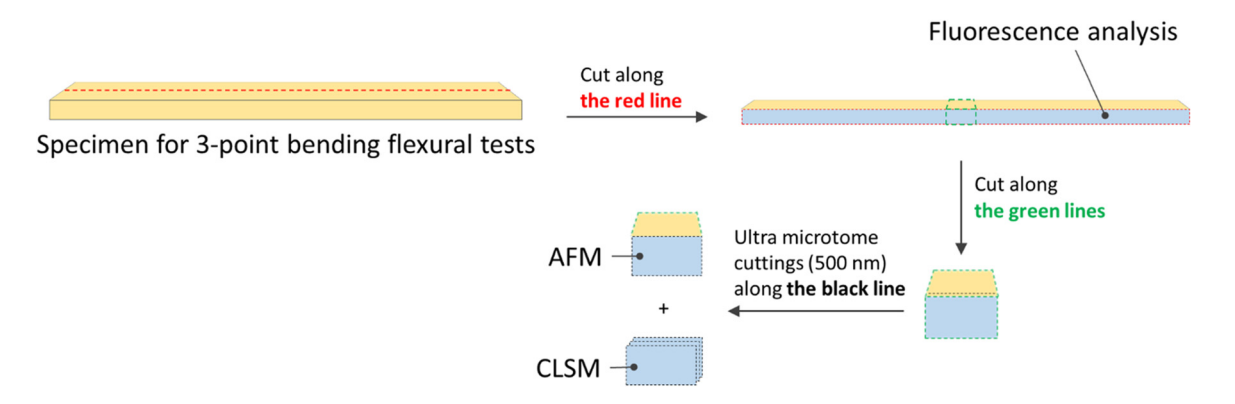


Figure 1: Cutting edges of the specimens for microscopic characterization.

fractions of lignin, which would not be present in the aminated lignins, were removed. Lignin (20 g) was dissolved in aqueous NaOH (0.2 M, 200 ml) and insoluble parts were removed via centrifugation (4500 rpm, 7 min) (3.2 g, 16%). Subsequently, the solution was treated with hydrochloric acid (2 M) to bring the pH value to 11.2. Then, the mixture was heated at 80 °C for 16 h. Consequently, the mixture was cooled to room temperature and the crude product was precipitated in a tenfold excess of isopropanol (2.5 l). The pre-treated lignin (KL) was separated via centrifugation (4700 rpm, 2 min) and was washed with isopropanol (2 × 500 ml). Finally, the product was suspended in isopropanol (1 l) and a sample (45 ml) was removed for further analysis. Yield: 8.18 g (41 wt.%) of the reference product KL. $M_w = 4735$ g mol⁻¹, $M_n = 2238 \text{ g mol}^{-1}$, Elemental analysis: C: 63.32%, H: 6.00%, N: 0.26%; OH number of KL was determined via 31P NMR of the phosphitylated compound according to the method of Argyropoulos (Granata and Argyropoulos 1995). OH number of guaiacylic OH was 1.80 mmol g⁻¹ and for *p*-hydroxyphenyl groups 0.29 mmol g⁻¹.

2.4 General protocol of lignin amination

The syntheses were accomplished following the protocol described elsewhere (Yue et al. 2011). Lignin (40 g) was dissolved in aqueous NaOH (0.2 M, 400 ml) and insoluble parts were removed via centrifugation (4500 rpm, 7 min) (6.4 g, 16%). Subsequently, the solution was treated with the desired amine (for individual amounts see descriptions below) and the pH value was brought to 11.2 by addition of hydrochloric acid. Then, formaldehyde (35% in water, 51 ml, 620 mmol) was added and the mixture was heated at 80°C for 20 h. Consequently, the mixture was cooled to room temperature and the crude product was precipitated in a tenfold excess of isopropanol (51) (anti-solvent precipitation). The product was separated via centrifugation (4700 rpm, 2 min) and the residue was washed with isopropanol $(2 \times 1 \text{ l})$. Finally, the product was suspended in isopropanol (1 l) to obtain stable microsuspensions of the aminated lignins. For further analysis a sample (45 ml) was collected. For details of all syntheses, see the Supplementary Material.

2.5 Preparation of the epoxy resin specimens

EPOSID 2031 (EEW 180–190), EPODUR VP664 (AE 58) and semi-dry lignin-isopropanol suspension (aminated lignin or KL) were mixed at $2500 \, \text{min}^{-1}$ in vacuo using a speedmixer for 30 min. The uncured resin

was filled into the previously prepared silicon forms (see Supplementary Material) (placed into 50 ml falcon tubes) and pressed into the forms with a centrifuge (4500 rpm, 22°C, 7 min) in multiple portions to obtain homogenous, void-free materials (lignin-free specimens were prepared by the same way but without addition of lignin). Subsequently, the resin-filled silicon forms were cured for 24 h at room temperature (22 °C) and further annealed for 4 h at 70 °C. After curing, the specimens could be easily removed from the silicon forms. As a reference experiment, the isopropanol was mainly replaced with acetone, which could easily be detected via FTIR spectroscopy (complete disappearance of the CO band at 1700 cm $^{-1}$). The properties of the resulting materials were similar.

2.6 Instruments and characterization methods

For microscopic analysis of the specimens, the samples were cut according to Figure 1.

3-point bending flexural tests were carried out on a Zwick/Roell zwickiLine Z1.0 TN with a 3-point flexure test kit according to DIN EN ISO 178 and ASTM D790 (DIN EN ISO 178 2017). The software testXpert II was used. The material was placed on two supports and deflected by applying force to the middle of the specimen with a tip (see supplementary material). A pre-force of 0.1 N, a testing speed of 10 mm min⁻¹ was applied according to DIN standards.

Atomic force microscopy (AFM): For the nanomechanical characterization of the lignin-based epoxy resins a Dimension Icon atomic force microscope (Bruker AXS, Santa Barbara, CA) in the PeakForce Tapping mode and RTESPA-300 silicon probes (nom. spring constant 40 N m⁻¹, tip radius 8 nm, purchased from the same company) were used. The inverse optical lever sensitivity and the spring constant were calibrated measuring the deflection in volts versus z-piezo position on stiff sapphire substrate, subsequently applying the thermal noise method. A maximum force of 15 nN was applied to the sample to obtain maps of the Young's modulus with 512×512 pixels resulting in a lateral resolution of approx. 10 nm. To this end, the sample was scanned with a velocity of 4 µm s⁻¹ while the cantilever was driven sinusoidally using an amplitude of 300 nm causing the tip to indent 2-5 nm into the sample surface to sense the force versus separation response of the sample. The retrace portion of each force versus separation curve was fitted by a Derjaguin-Muller-Toporov (DMT) model to extract the local elasticity values at the respective sample positions (Butt and Jaschke 1995).

Confocal laser scanning microscopy (CLSM) was carried out using a Leica TCS SP8 CLSM. The sample, together with a small amount of water, was placed between two coverslips. Fluorescence was excited with 365 nm laser light and fluorescence excitation was detected between 450 and 600 nm with a HyD detector using a 63× water immersion objective (HC PL APO CS2 63×/1.20 WATER). The confocal pinhole was set to 0.7 airy units.

Fluorescence mapping was performed with a Vilber Fusion FX with an excitation wavelength of 365 nm and mapping of the emission at 535 nm.

Infrared (IR) spectroscopy was performed on a PerkinElmer Instruments Systems One FT-IR Spectrometer, coupled to a universal attenuated total reflectance (UATR) unit. Ten scans were recorded per measurement with a resolution of 4 cm⁻¹, between wavenumbers of 4000 and 650 cm⁻¹. For each sample, an average spectrum was formed from 2 of these individual measurements. The software Spectrum Version 6.3.5.0177 Copyright® 2009 PerkinElmer Inc. was used. A mathematical manipulation like baseline correction or normalization of the spectra was not performed.

Microtome cuttings were performed using a Leica Ultracut R (Leica Biosystems, Nußloch, Germany).

Nuclear magnetic resonance (NMR) spectroscopy: NMR spectroscopy was performed on a Bruker AC300 (300 MHz). Chemical shifts are shown in parts per million (ppm). Quantitative ³¹P spectra are reported in δ units, ppm downfield from phosphoric acid (H_3PO_4) and are calibrated by addition of endo-N-hydroxy-5-norbornene-2,3-dicarboximide as internal standard (Zawadzki and Ragauskas 2001). The software MestReNova Version 11.0 (Mestrelab Research S.L.) was used.

Size exclusion chromatography (SEC) were performed with a 1260 Infinity GPC/SEC system from Agilent Technologies. The columns used were MCX HS 1000A (# 5120913) and MCX HS 100000 (#91091811) at 25°C. The concentrations of the samples were about 2 mg in 1 ml of buffer solution (0.1% of ethylene glycol in 0.1 M aqueous NaOH) with a flow rate of 1 ml min⁻¹, an injection volume of 20 µl and aqueous NaOH (0.1 M) as eluent. The calibration was performed against polystyrene sulfonate. A 1260 RID detector was

Vacuo mixing: epoxy formulations were prepared in a Hauschild & Co KG Speedmixer DAC 400.2 VAC-P Software version V25.

3 Results and discussion

The successful reaction of kraft lignin with the four model amine compounds (DETA, PDA, EDA and NH₃) was demonstrated via IR spectroscopy (see Figure 2). In the spectra of the aminated lignins KL-DETA, KL-PDA and KL-EDA a significant signal at 1640-1680 cm⁻¹ could be observed (see Figure 2). This signal can be attributed to the NH deformation vibrational band of the amino groups. In case of KL-NH3 only a very small signal could be observed, because it provides no primary amino groups and the introduced amount of amines is relatively low. In order to demonstrate qualitatively that the above mentioned signal can be attributed to a nitrogen species, and because the signal overlaps with a lignin-intrinsic signal at 1600 cm⁻¹,

the amino groups were protonated/acidified by placing the samples into an exsiccator together with a flask containing concentrated hydrochloric acid (35%) for 24 h at 22 °C and IR spectra were captured before and after acidification. By this, significant changes could be observed in all cases (see

In order to receive quantitative information about the modification of the arenes, the lignin derivatives were further analyzed through the total nitrogen content determined by elemental analysis (see Table 1). As expected, the lowest amount of amine molecules was introduced into lignin by using ammonia (1.2 mmol g⁻¹). The reason for this can be attributed to the fact that the benzoxazine species generated by the Mannich reaction of lignin with ammonia, is more prone for the formation of the Mannich base, due to its higher reactivity, in comparison to the other model amines used in this study. Consequently, intramolecular crosslinking may occur with KL-NH3 at a higher extent, and less reactive positions remain for introduction of further ammonia molecules. In total, 2.2 mmol g⁻¹ guaiacyl and p-hydroxyphenyl positions were available for functionalization, as determined by ³¹P NMR. The further trend of the introduced amine moieties with DETA, PDA and EDA, respectively, follows closely the chain lengths of the spacers with respect to their reactivity: Once the amines are bound to the arenes of the lignin, the longer DETA moieties are sterically less hindered, and thus, undergo crosslinking to a higher extent (leading to the introduction of less amine moieties: 1.7 mmol g⁻¹), whereas in KL-PDA and KL-EDA slightly less crosslinking occurs because of higher steric hindrance of the lignin-bound amines. Therefore, 1.8 and 2.0 mmol g⁻¹ amine molecules were introduced during the amination reaction (see Table 1). Here it was assumed that the extent of intermolecular crosslinking can be neglected, since the molecular mass (number average M_n as determined by size exclusion chromatography SEC) of all aminated lignins were of the same order of magnitude as the nonmodified kraft lignin, respectively ($M_{n,KL} = 2200 \text{ g mol}^{-1}$; $M_{n,\text{KL-DETA}} = 2700 \text{ g mol}^{-1}; M_{n,\text{KL-PDA}} = 2700 \text{ g mol}^{-1};$ $M_{n,\text{KL-EDA}} = 2200 \text{ g mol}^{-1}; M_{n,\text{KL-NH3}} = 2700 \text{ g mol}^{-1})$ (see Table 1). The increase of the M_w during the amination procedure at almost constant M_n indicates that only a small amount of the molecules undergoes intermolecular crosslinking reactions, whereas the majority preserved the initial molecular weight (see Table 1).

Because of the low solubility of the aminated lignins, further elucidation of the chemical structure, e.g. by NMR spectroscopy is highly challenging and might only be possible if sophisticated solid state 2DNMR experiments are being applied.

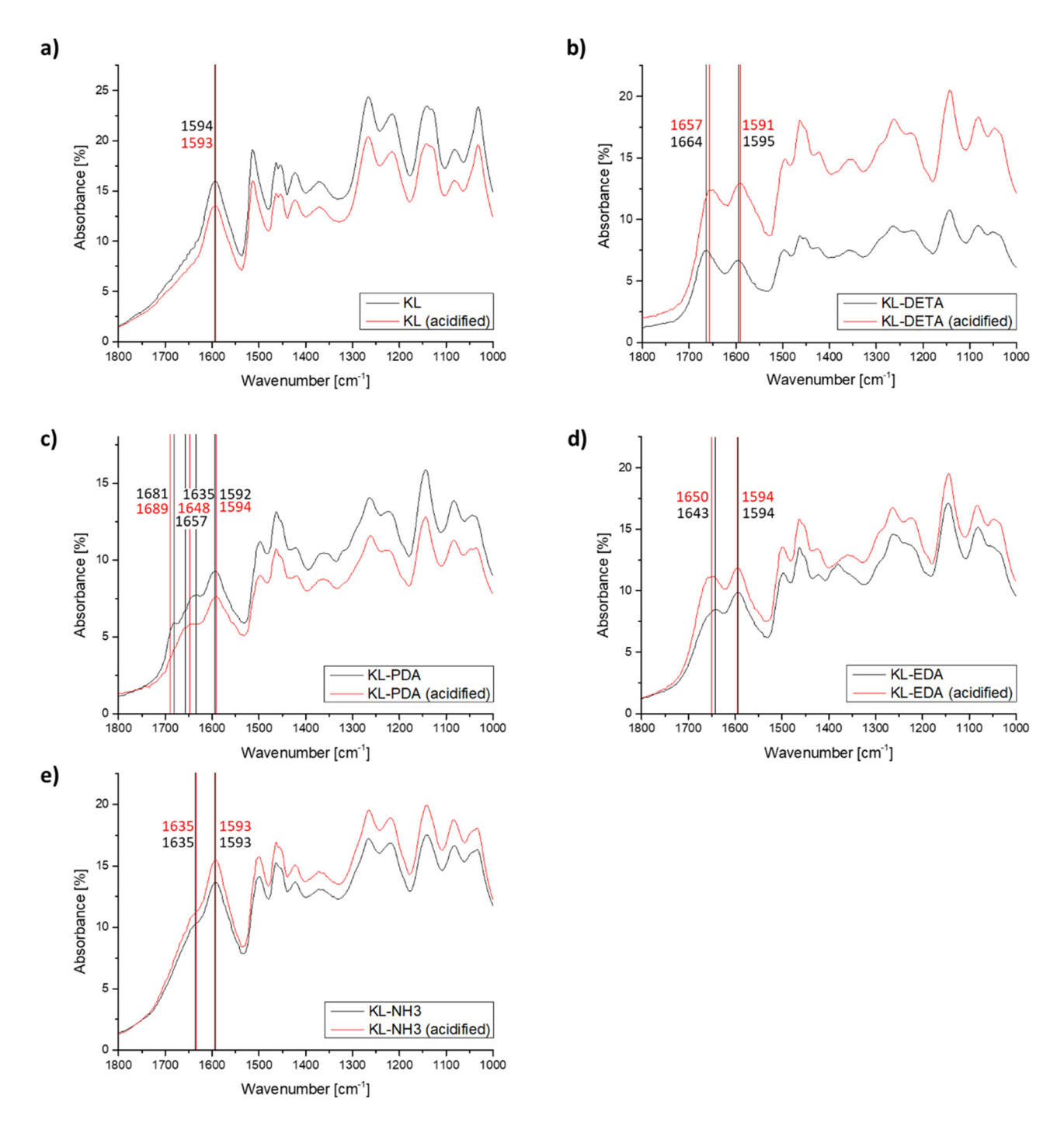


Figure 2: IR spectra of the different acidified (red line) and non-acidified (black line) lignin derivatives.

In the next step, these compounds were used for hardening of a cold-curing BADGE (bisphenol A diglycidyl ether)-based epoxy resin (EEW 180–190). In order to ensure a large reactive interface, and thus, a strong bond between lignin and the epoxy compound, the lignins were incorporated as microsuspensions obtained by anti-solvent precipitation. By mixing the compounds in vacuo the nonsolvent as well as any gases were removed and the lignin

particles were surrounded by the epoxy compound (see Supplementary Material). Since it was important in this procedure that the surrounding medium could be easily removed in vacuum, whereas the shape and the stability of the particles played a minor role, the lignins were precipitated directly from the reaction mixture (dissolved in aqueous 0.2 M NaOH) into isopropanol as a non-solvent (followed by washing with isopropanol) instead of using

Table 1: Overview of key features/parameters of the different synthesized aminated lignins.

Amine	<i>M_n</i> of aminated lignin (g mol⁻¹)	<i>M_w</i> of aminated lignin (g mol⁻¹)	Amount of introduced amine molecules (mmol g ⁻¹)°	Homo crosslinking features
None (KL)	2200	4700	0	`{_O\`
Diethylene triamine (DETA)	2700	28,100	1.7 (77%) ^b	N N N N N N N N N N N N N N N N N N N
				KL-DETA
Propylene diamine (PDA)	2700	11,700	1.8 (81%) ^b	KL-PDA
Ethylene diamine (EDA)	2200	14,400	2.0 (91%) ^b	KL-EDA AMERICA
Aqueous solution of ammonia	2700	9100	1.2 (55%) ^b	KL-NH3 OH

Determined by using the total nitrogen content via elemental analysis (see Supplementary Material). Molecular yields: 2.2 mmol g-1 of guaiacyl and p-hydroxyphenyl positions are potentially available for functionalization.

methods requiring water as a non-solvent or addition of any surfactants (Lievonen et al. 2016; Lintinen et al. 2018; Nypelö et al. 2015; Sipponen et al. 2017, 2018).

Although curing of the oxiranes exclusively with the aminated lignins is possible, an additional curing agent was added (polyether amine, AE 58), as otherwise the viscosity of the mixture became too high to prepare homogeneous specimens in a reproducible fashion. Therefore, an optimized amount of 23 wt.% of lignin, 38.5 wt.% epoxy compound and 38.5 wt.% polyether-amine was used for all formulations. For preparation of the specimens, the uncured, highly viscous mixtures were filled into vertical silicon forms via centrifugal molding and cured for 24 h at 22 °C followed by a thermal posttreatment for 4 h at 70 °C (see Supplementary Material). In this way, a reliable preparation of void-free and odor-less specimens with very accurate dimensions was possible.

Centrifugation or wall-effects may interfere with lignin distribution in the specimen, therefore the cross-section of the samples was analyzed with respect to their lignin autofluorescence in detail. Samples were cut in the middle, illuminated with UV light (365 nm) and the autofluorescence intensity (at 535 nm) was mapped and analyzed by quantitative greyscale analysis (see Figure 3a and b). As a result, all specimens investigated provide a highly homogeneous macroscopic lignin distribution and no concentration gradients or lignin agglomeration could be observed. Furthermore, microtome cuttings (500 nm) were prepared from the inside of the samples and analyzed by confocal laser scanning microscopy (CLSM, see Figure 3c). In these micrographs, the auto-fluorescent lignin particles could be distinctly discriminated from the polymer matrix and are present as well-defined phase-separated domains, which are homogeneously distributed. The size of these domains is below ~200 nm, and thus, below the resolution limit of the microscope. This is consistent with the particle sizes of the lignins, which were determined separately by SEM of the microsuspension, before incorporation into the polymer (see Supplementary Material).

Finally, the mechanical properties of the specimens were determined macroscopically via 3-point bending flexural tests according to DIN EN ISO 178 (see Figure 4).

All specimens of the aminated lignins exhibit a high flexural strengths of 69-75 MPa, the flexural strength of reference lignin (KL) is distinctly lower (57 MPa) (Figure 4a).

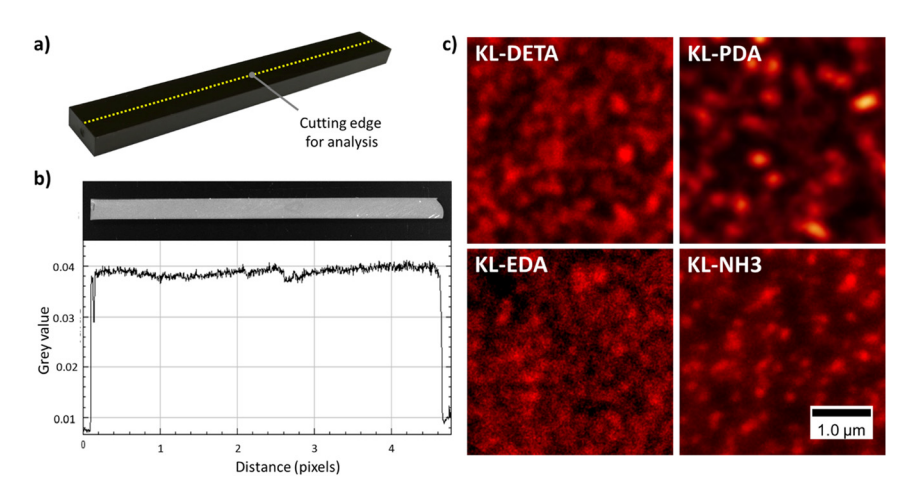


Figure 3: (a) Photograph of a test specimen (cutting edge is indicated as a yellow dashed line); (b) fluorescence image and grey value of the cutting edge of a typical test specimen (e.g., KL-PDA-based resin); (c) CLSM images of epoxy resin slices (500 nm film thickness) made of different aminated lignins (samples were taken from the center of the specimens).

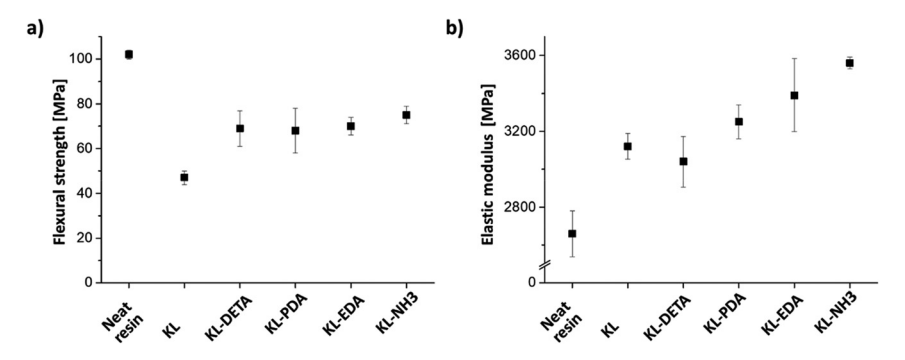


Figure 4: (a) Flexural strengths and (b) elastic modules of the resins made of different lignins determined according to DIN standards (DIN EN ISO 178 2017).

Regarding the flexibility, as hypothesized, the KL-NH3-based resin provides the highest elastic modulus (EKL-NH3 $_{\rm resin}$ = 3560 MPa) because KL-NH3 exhibits the highest degree of crosslinking as well as the most rigid molecular structure. Interestingly, the tendency of the elastic modulus of the remaining lignins follows the order of molecular flexibilities, which obviously overcomes the

influence of the degree of crosslinking: The material made of KL-DETA possesses the lowest modulus (3040 MPa) (this value is similar to the modulus of the unmodified KL-based material [3050 MPa]) followed by the KL-PDA ($E_{\rm KL-PDA}$) followed by the KL-PDA ($E_{\rm KL-PDA}$) and KL-EDA-based resins ($E_{\rm KL-EDA}$) (see Figure 4b). Because the macroscopic measurements depend on a plethora of

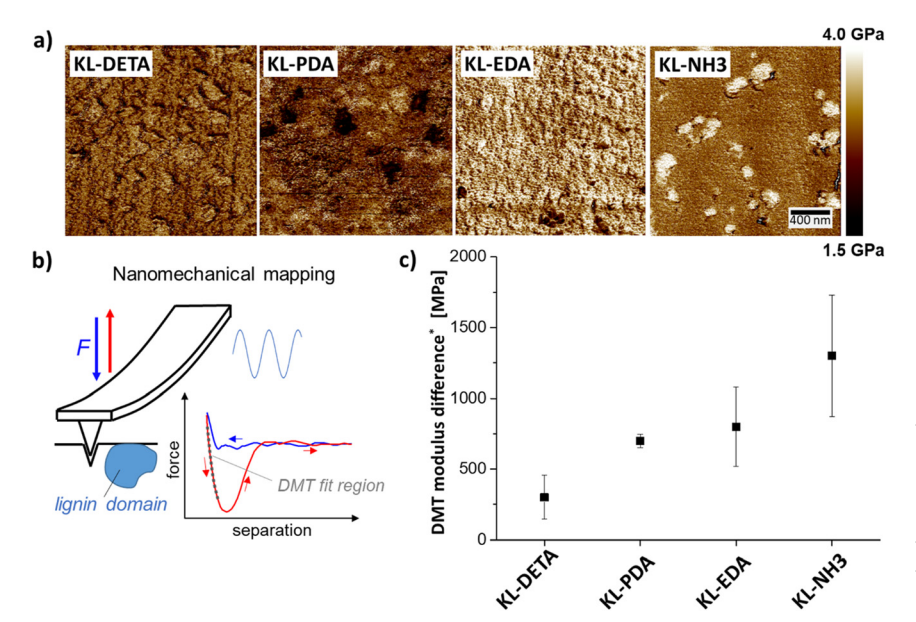


Figure 5: (a) Nanomechanical mappings of the epoxy resins made by using the different lignins determined via AFM PeakForce tapping; (b) schematic of the measurement principle; (c) differences of the DMT modules of the lignin domains and the matrix polymer within the cured resins, determined by AFM PeakForce tapping.

further influencing factors (e.g. geometry of the lignin domains), the elastic properties of the lignin domains were measured in a spatially resolved manner by AFM in order to demonstrate that the lignin-intrinsic properties of the resins prepared follow the exact same trend.

To this end, the DMT modules (Young's modules determined by using the Derjaguin, Muller, Toropov model) of the cut surfaces of the resins were mapped by AFM using the PeakForce tapping modus (see Figure 5b). As can be inferred from the micrographs, lignin domains can easily be discriminated from the matrix resin as areas with increased rigidity (see Figure 5a). Subsequently, the DMT modules of the lignin domains as well as the surrounding polymer matrix were quantified under similar conditions and the differences of the DMT modules of the lignin domains and the matrix polymer were determined for each sample (see Figure 5c) (note that it is not possible to compare the DMT modulus of reference samples made of KL with the values made of aminated lignins, because KL domains provide a distinctly lower integrity, which implies rough and inhomogeneous surfaces. Furthermore, the non-covalently bound KL domains are soluble in water, which further makes it difficult to prepare suitable surfaces). As hypothesized, the AFM measurements showed the same trend, if compared to flexural tests at the macroscopic scale: The modulus of the lignin domains in the KL-NH₃-based resin was the highest, followed by the resins made of KL-EDA, KL-PDA and finally KL-DETA. These results demonstrate that the macroscopic elastic moduli are predominantly determined by the intrinsic elasticity of the lignin domains, rather than from other parameters, such as geometrical effects.

4 Conclusion

In conclusion, it was demonstrated that the molecular structure of the amine, which is used for amination of lignin via Mannich reaction, has a significant impact on the elastic properties of epoxy resins made of such functional lignins. In-depth AFM studies indicate that elastic moduli of the cured lignin-epoxy resin are mainly governed by the intrinsic elasticity of the lignin domains within the resin. The latter can thus be controlled by the molecular flexibility of the amines. The work thus contributes to a better understanding of the relationship between molecular structure of functionalized lignin and the macroscopic mechanical properties of lignin-based resins made thereof, and thus enables a controlled tailoring of the elastic properties of lignin-based epoxy resins.

Acknowledgements: The authors thank Heike Herbert and Markus Langhans for valuable technical support.

Author contribution: All the authors have accepted responsibility for the entire content of this submitted manuscript and approved submission.

Research funding: This project has received funding from the Bio Based Industries Joint Undertaking under the European Union's Horizon 2020 research and innovation programme under grant agreement no. 669065 (ValChem). The manuscript reflects only the author's view and the JU is not responsible for any use that may be made of the information it contains.

Conflict of interest statement: The authors declare no conflicts of interest regarding this article.

References

- Abarro, G.J., Podschun, J., Diaz, L.J., Ohashi, S., Saake, B., Lehnen, R., and Ishida, H. (2016). Benzoxazines with enhanced thermal stability from phenolated organosolv lignin. RSC Adv. 6: 107689-107698.
- Auvergne, R., Caillol, S., David, G., Boutevin, B., and Pascault, J.-P. (2014). Biobased thermosetting epoxy: present and future. Chem. Rev. 114: 1082-1115.
- Brezny, R., Paszner, L., Micko, M. M., and Uhrin, D. (1988). The ionexchanging lignin derivatives prepared by mannich reaction with amino acids. Holzforschung 42: 369-373.
- Burke, W.J. (1949). 3,4-Dihydro-1,3,2H-benzoxazines. Reaction of p-substituted phenols with N,N-dimethylolamines. J. Am. Chem. Soc. 71: 609-612.
- Butt, H.-J. and Jaschke, M. (1995). Calculation of thermal noise in atomic force microscopy. Nanotechnology 6: 1-7.
- Crestini, C., Lange, H., Sette, M., and Argyropoulos, D.S. (2017). On the structure of softwood kraft lignin. Green Chem. 19: 4104-4121.
- Danielson, B. and Simonson, R. (1998). Kraft lignin in phenol formaldehyde resin. Part 1. Partial replacement of phenol by kraft lignin in phenol formaldehyde adhesives for plywood. J. Adhes. Sci. Technol. 12: 923-939.
- DIN EN ISO 178. (2017). Plastics determination of flexural properties (ISO/DIS 178:2017).
- Ding, C. and Matharu, A.S. (2014). Recent developments on biobased curing agents: a review of their preparation and use. ACS Sustain. Chem. Eng. 2: 2217-2236.
- Ding, N., Wang, X., Tian, Y., Yang, L., Chen, H., and Wang, Z. (2014). A renewable agricultural waste material for the synthesis of the novel thermal stability epoxy resins. Polym. Eng. Sci. 54:
- Ge, Y., Song, Q., and Li, Z. (2015). A Mannich base biosorbent derived from alkaline lignin for lead removal from aqueous solution. J. Ind. Eng. Chem. 23: 228-234.
- Gioia, C., Lo Re, G., Lawoko, M., and Berglund, L. (2018). Tunable thermosetting epoxies based on fractionated and wellcharacterized lignins. J. Am. Chem. Soc. 140: 4054-4061.
- Granata, A. and Argyropoulos, D.S. (1995). 2-Chloro-4,4,5,5-tetramethyl-1,3,2-dioxaphospholane, a reagent for the

- accurate determination of the uncondensed and condensed phenolic moieties in lignins. J. Agric. Food Chem. 43: 1538-1544.
- Guo, Z.-X. and Gandini, A. (1991). Polyesters from lignin-2. The copolyesterification of kraft lignin and polyethylene glycols with dicarboxylic acid chlorides. Eur. Polym. J. 27: 1177-1180.
- Guo, Z.-X., Gandini, A., and Pla, F. (1992). Polyesters from lignin. 1. The reaction of kraft lignin with dicarboxylic acid chlorides. Polym. Int. 27: 17-22.
- Hofmann, K. and Glasser, W.G. (2006). Engineering plastics from lignin. 22. Cure of lignin based epoxy resins. J. Adhes. 40: 229-241.
- Jiang, L., Li, S., Li, X., Li, Z., and Wang, X. (2013). Preparation of aminolignin from paper mill sludge and its discolouring flocculant performance. Asian J. Chem. 25: 1279-1284.
- Laobuthee, A., Chirachanchai, S., Ishida, H., and Tashiro, K. (2001). Asymmetric mono-oxazine: an inevitable product from mannich reaction of benzoxazine dimers. I. Am. Chem. Soc. 123: 9947-9955.
- Laurichesse, S. and Avérous, L. (2014). Chemical modification of lignins: towards biobased polymers. Prog. Polym. Sci. 39: 1266-1290.
- Lievonen, M., Valle-Delgado, J.J., Mattinen, M.-L., Hult, E.-L., Lintinen, K., Kostiainen, M.A., Paananen, A., Szilvay, G.R., Setälä, H., and Österberg, M. (2016). A simple process for lignin nanoparticle preparation. Green Chem. 18: 1416-1422.
- Lintinen, K., Xiao, Y., Bangalore Ashok, R., Leskinen, T., Sakarinen, E., Sipponen, M., Muhammad, F., Oinas, P., Österberg, M., and Kostiainen, M. (2018). Closed cycle production of concentrated and dry redispersible colloidal lignin particles with a three solvent polarity exchange method. Green Chem. 20: 843-850.
- Liu, J., Liu, H.-F., Deng, L., Liao, B., and Guo, Q.-X. (2013). Improving aging resistance and mechanical properties of waterborne polyurethanes modified by lignin amines. J. Appl. Polym. Sci. 130: 1736-1742.
- Mendis, G.P., Hua, I., Youngblood, J.P., and Howarter, J.A. (2015). Enhanced dispersion of lignin in epoxy composites through hydration and mannich functionalization. J. Appl. Polym. Sci. 132: 121.
- Mikawa, H., Sato, K., Takasaki, C., and Ebisawa, K. (1956). Mannich reaction on lignin model compounds and the estimation of the amount of the simple guaiacyl nucleus in thiolignin. Stud. Cook. Mech. Wood XV: 29, 259-265.
- Moorer, H.H., Dougherty, W.K., and Ball, F.J. (1970). Method of Producing Synthetic Lignin-Polyisocyanate Resin. US Patent 3.519.581. Westvaco Corporation.
- Newmann, W.H. and Glasser, W.G. (1985). Engineering plastics from lignin. Holzforschung 39: 345-353.
- Nieh, W.L.-S. and Glasser, W.G. (1989). Lignin epoxide. In: Glasser, W.G. and Sarkanen, S. (Eds.), Lignin. Washington, DC: American Chemical Society, pp. 506-514.
- Nypelö, T.E., Carrillo, C.A., and Rojas, O.J. (2015). Lignin supracolloids synthesized from (W/O) microemulsions: use in the interfacial stabilization of Pickering systems and organic carriers for silver metal. Soft Matter 11: 2046-2054.
- Pan, H., Sun, G., and Zhao, T. (2013). Synthesis and characterization of aminated lignin. Int. J. Biol. Macromol. 59: 221-226.
- Phalak, G.A., Patil, D.M., and Mhaske, S.T. (2017). Synthesis and characterization of thermally curable guaiacol based

- poly(benzoxazine-urethane) coating for corrosion protection on mild steel. Eur. Polym. J. 88: 93-108.
- Ragauskas, A.J., Beckham, G.T., Biddy, M.J., Chandra, R., Chen, F., Davis, M.F., Davison, B.H., Dixon, R.A., Gilna, P., Keller, M., et al. (2014). Lignin valorization: improving lignin processing in the biorefinery. Science (New York, N.Y.) 344: 1246843.
- Sasaki, C., Wanaka, M., Takagi, H., Tamura, S., Asada, C., and Nakamura, Y. (2013). Evaluation of epoxy resins synthesized from steam-exploded bamboo lignin. Ind. Crop. Prod. 43: 757-761.
- Sipponen, M.H., Lange, H., Ago, M., and Crestini, C. (2018). Understanding lignin aggregation processes. A case study: budesonide entrapment and stimuli controlled release from lignin nanoparticles. ACS Sustain. Chem. Eng. 6: 9342-9351.
- Sipponen, M.H., Smyth, M., Leskinen, T., Johansson, L.-S., and Österberg, M. (2017). All-lignin approach to prepare cationic colloidal lignin particles: stabilization of durable Pickering emulsions. Green Chem. 19: 5831-5840.
- Sun, J., Wang, C., Stubbs, L.P., and He, C. (2017). Carboxylated lignin as an effective cohardener for enhancing strength and toughness of epoxy. Macromol. Mater. Eng. 302: 1700341.
- Sun, Z., Fridrich, B., Santi, A., de Elangovan, S., and Barta, K. (2018). Bright side of lignin depolymerization: toward new platform chemicals. Chem. Rev. 118: 614-678.
- Tejado, A., Peña, C., Labidi, J., Echeverria, J.M., and Mondragon, I. (2007). Physico-chemical characterization of lignins from different sources for use in phenol-formaldehyde resin synthesis. Bioresour. Technol. 98: 1655-1663.
- Türk, O. (2014). Stoffliche Nutzung nachwachsender Rohstoffe. Wiesbaden: Springer Fachmedien Wiesbaden.
- Upton, B.M. and Kasko, A.M. (2016). Strategies for the conversion of lignin to high-value polymeric materials: review and perspective. Chem. Rev. 116: 2275-2306.
- Yue, X., Chen, F., and Zhou, X. (2011). Improved interfacial bonding of PVC/wood-flour composites by lignin amine modification. BioResources 6: 2022-2034.
- Zawadzki, M. and Ragauskas, A. (2001). N-hydroxy compounds as new internal standards for the 31P-NMR determination of lignin hydroxy functional groups. Holzforschung 55: 175.
- Zhang, R., Xiao, X., Tai, Q., Huang, H., and Hu, Y. (2012). Modification of lignin and its application as char agent in intumescent flame-retardant poly(lactic acid). Polym. Eng. Sci. 52: 2620-2626.
- Zhao, S., Huang, X., Whelton, A.J., and Abu-Omar, M.M. (2018). Formaldehyde-free method for incorporating lignin into epoxy thermosets. ACS Sustain. Chem. Eng. 6: 10628-10636.
- Zieglowski, M., Trosien, S., Rohrer, J., Mehlhase, S., Weber, S., Bartels, K., Siegert, G., Trellenkamp, T., Albe, K., and Biesalski, M. (2019). Reactivity of isocyanate-functionalized lignins: a key factor for the preparation of lignin-based polyurethanes. Front. Chem. 7: 15.

Supplementary Material: Supplementary material to this article can be found online at https://doi.org/10.1515/hf-2020-0060.